Raman Suppression and All-Optical Control in Media With a Zero-Nonlinearity Wavelength

Alexis C. Sparapani, *Member, IEEE*, Lucas N. Gutierrez, Santiago M. Hernandez, Pablo I. Fierens, *Senior Member, IEEE*, Diego F. Grosz, and Govind P. Agrawal, *Life Fellow, IEEE*

***Abstract*— We study the interaction between an intense soliton and a weak control pulse in optical media with a zero-nonlinearity wavelength (ZNW). By means of numerical simulations, we show that the soliton's wavelength and group delay can be modified by a proper choice of parameters of the control pulse, such as its power, frequency, and initial delay. Most remarkably, we demonstrate either the suppression of the soliton's Raman-Induced Frequency Shift (RIFS) or the enhancement of this effect and explain it by temporal analogies of reflection and transmission. Finally, we propose an all-optical switching scheme based on time and frequency windows.**

***Index Terms*— Nonlinear optics, all-optical switching, zero-nonlinearity wavelength, temporal analogy.**

I. Introduction

ALL-OPTICAL control enables one to take advantage of broad bandwidth, immunity to electromagnetic radiation, and ultra-fast processing [1], [2], and it has applications in many areas, including signal processing [3], [4], sensing [5], [6], [7], and switching [8], [9], [10], among others. Most frequently, all-optical control schemes rely on the interaction between two pulses. Parameters of one pulse, such as its width and power [11], delay [12], chirp [13], wavelength [14], and sharpness [15] can be tuned in order to exert control over the second pulse in a desired way.

Manuscript received 17 January 2024; revised 16 May 2024; accepted 28 June 2024. Date of publication 8 July 2024; date of current version 17 July 2024. This work was supported in part by CONICET under project PIP 2021 11220200100566CO. *(Corresponding author: Alexis C. Sparapani.)*

Alexis C. Sparapani was with Grupo de Comunicaciones Òpticas, Departamento de Ingeniería en Telecomunicaciones, Instituto Balseiro, Comisión Nacional de Energía Atómica, Bariloche R8400, Argentina, and also with Consejo Nacional de Investigaciones Científicas y Técnicas (CONICET), Buenos Aires C1425, Argentina. He is now with the Department of Information Engineering, Electronics and Telecommunications, Sapienza University of Rome, 00184 Rome, Italy (e-mail: acsparapani@ib.edu.ar).

Lucas N. Gutierrez, Santiago M. Hernandez, and Diego F. Grosz are with Grupo de Comunicaciones Ópticas, Departamento de Ingeniería en Telecomunicaciones, Instituto Balseiro, Comisión Nacional de Energía Atómica, Bariloche R8400, Argentina, and also with Consejo Nacional de Investigaciones Científicas y Técnicas (CONICET), Buenos Aires C1425, Argentina.

Pablo I. Fierens is with Centro de Optoelectrónica, Instituto Tecnológico de Buenos Aires (ITBA), Buenos Aires C1437, Argentina, and also with CONICET, Buenos Aires C1425, Argentina.

Govind P. Agrawal is with the Institute of Optics, University of Rochester, Rochester, NY 14627 USA.

Color versions of one or more figures in this article are available at https://doi.org/10.1109/JQE.2024.3424417.

Digital Object Identifier 10.1109/JQE.2024.3424417

Temporal analogies of the reflection and refraction phenomena, including the case of total internal reflection (TIR), are oftentimes useful to analyze the interaction of optical pulses [16]. In fact, they have been recently used in the study of pulse splitting [17] and deceleration [18], distributed sensing [19], and all-optical switching [12].

In this work, we focus on the interaction of optical pulses in waveguides with a frequency-dependent nonlinearity, which can be achieved, for instance, by doping with metal nanoparticles or by the use of metamaterials [20]. This type of waveguides exhibit a zero-nonlinearity wavelength (ZNW), around which the nonlinear parameter switches its sign [21], [22]. Recently, it has been studied how the ZNW and its position relative to the zero-dispersion wavelength (ZDW) affect the propagation dynamics of a pulse [21], [23], [24], [25] and the interaction between two different pulses [26]. In [26] the influence of a ZNW on the frequency shift and the delay of a soliton interacting with a weaker control pulse is studied. The analysis, based on the temporal analogy of reflection and refraction, pointed to engineering rules for the all-optical control of a soliton; however, the influence of Raman scattering was not taken into account. In this work, we extend the analysis in [26] to more general conditions, explicitly accounting for the effect of Raman scattering and discussing the role of a ZNW within this context. We study how controllable parameters of the control pulse such as its power, wavelength, and initial delay affect the soliton. Most noteworthy, we show that the control pulse can be used to either enhance or suppress the Raman frequency shift experienced by the intense soliton, as pictorially depicted in Fig. 1. Finally, we propose an all-optical switching scheme whereby the tuning of easily addressable parameters of the control pulse is shown to allow the control of the frequency and delay of the soliton.

Our study is organized as follows: In Section II we present the propagation equations used for the ensuing analysis. Section III studies the influence of the ZNW and the parameters of the control pulse over the soliton, along with remarks regarding the application to all-optical switching. Finally, Section IV presents our conclusions.

II. Propagation Equations

It must be emphasized that pulse propagation in media with an arbitrary frequency-dependent nonlinear response cannot

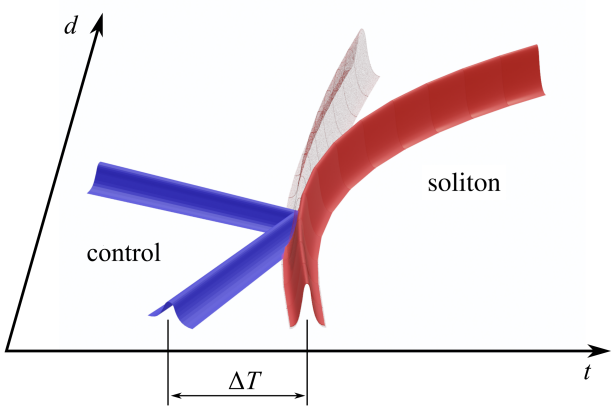

Fig. 1. Schematic representation of a soliton controlled by a low-intensity dispersive pulse through temporal reflection. The gray part shows soliton's trajectory in the absence of the control pulse.

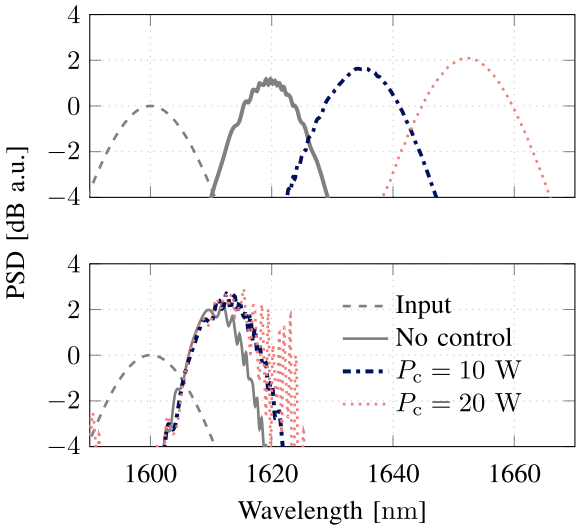

Fig. 2. Output soliton spectrum under several different conditions for ZNW = 1450 nm (top) and ZNW = 1650 nm (bottom). The control pulse delay is $\Delta T = -7.5$ ps.

be tackled with the usual generalized nonlinear Schrödinger equation (GNLSE) [27]. Indeed, it is well known that the GNLSE may yield unphysical solutions which do not conserve the number of photons in lossless waveguides [28]. Thus, for our analysis we turn to the photon-conserving generalized nonlinear Schrödinger equation (pcGNLSE) [29], which addresses the problem of photon-number conservation when dealing with such nonlinearity profiles. Moreover, this equation includes the effect of intrapulse Raman scattering, which becomes non-negligible for pulses shorter than 1 ps [2]. The pcGNLSE can be written in the frequency domain as

$$\partial_z \tilde{A} = i\beta(\Omega)\tilde{A} + i\frac{\Gamma(\Omega)}{2}\mathcal{F}\left\{C^* B^2\right\} + i\frac{\Gamma^*(\Omega)}{2}\mathcal{F}\left\{B^* C^2\right\} + i f_R \Gamma^*(\Omega)\mathcal{F}\left\{B\int_0^\infty h_R(t')|B(t-t')|^2 dt' - B|B|^2\right\}, \tag{1}$$

where $\tilde{A}(z,\Omega)$ is the Fourier transform of the complex envelope of the electrical field, $\beta(\Omega)$ is the dispersion profile, $\mathcal{F}$ is the Fourier-transform operator, $h_R(t)$ accounts for the delayed Raman response, and f_R is the fractional Raman contribution. The fields B, C and the modified nonlinear profile Γ are defined in the frequency domain as

$$2\tilde{B}(z,\Omega) = r(\Omega)\tilde{A}(z,\Omega), \quad \tilde{C}(z,\Omega) = r^*(\Omega)\tilde{A}(z,\Omega), \tag{2}$$

$$r(\Omega) = \sqrt[4]{\frac{\gamma(\Omega)}{\omega_0+\Omega}}, \quad \Gamma(\Omega) = \sqrt[4]{\gamma(\Omega)\cdot(\omega_0+\Omega)^3}, \tag{3}$$

with $\Omega = \omega - \omega_0$, where ω_0 is the soliton central frequency in the ensuing analysis, and the nonlinear parameter $\gamma(\Omega)$ is defined as in [27]. In this work, we assume a linear dependence of $\gamma(\Omega)$ with frequency

$$\gamma(\Omega) = \gamma_0 + \gamma_1(\Omega) = \gamma_0\left(1 + s\frac{\Omega}{\omega_0}\right), \tag{4}$$

where s is the self-steepening parameter.

The propagation of solitons under the pcGNLSE has been extensively studied [24], [30], [31], [32]. In particular, in [31] it was shown that the frequency shift and delay experienced by a soliton due to Raman scattering are given by

$$\delta\Omega_p = \frac{-8T_R\gamma_0 P_0}{15T_0^2}z, \; \delta T_p = \frac{\beta_2\Omega_p}{2}z + \frac{(s+2)\gamma_0 P_0}{3\omega_0}z, \tag{5}$$

where P_0 is the pulse peak power, T_0 the $1/e$ time width, T_R is the effective Raman parameter [27], and β_2 is the group velocity dispersion parameter of the waveguide. In the following section, we shall show that both the frequency and delay experienced by the soliton upon propagation can be controlled, and even suppressed or enhanced, through its interaction with a control pulse of a considerably lower power.

III. All-Optical Control of the Soliton

We study the interaction between an intense soliton and a weaker control pulse by means of numerical simulations. In all cases, we launch an 85-fs fundamental soliton at $\lambda_0 = 1600$ nm with a peak power $P_0 = 243.6$ W, along with a 2.1-ps sech control pulse with peak power P_c, at the input of a 300-m-long fiber with dispersion parameters $\beta_2 = -4.4$ ps^2 km^{-1} and $\beta_3 = 0.13$ ps^3 km^{-1}, resulting in a ZDW at 1555 nm and placing the intense pulse in the anomalous dispersion region. The zeroth-order nonlinear coefficient was set to $\gamma_0 = 2.5$ W^{-1} km^{-1} and the first-order nonlinear coefficient γ_1 was varied in order to set the ZNW to either 1450 or 1650 nm. The dispersion and nonlinear coefficients are defined for the soliton's wavelength. Fiber losses were neglected by assuming that the propagation distance is shorter than the fiber's effective length.

Figure 2 compares the soliton spectrum with and without a control pulse, launched at $\lambda_c = 1522$ nm and delayed from the soliton by -7.5 ps, using $P_c = 10$ and 20 W. Under the space-time analogy, the soliton acts as a barrier for the weaker dispersive pulse. Since there is no interaction between both pulses in the case of total transmission, the control pulse must (at least partially) be reflected by the soliton, noting that there is no reflection whenever the ZNW lies between control and soliton wavelengths [26]. As such, we present results for

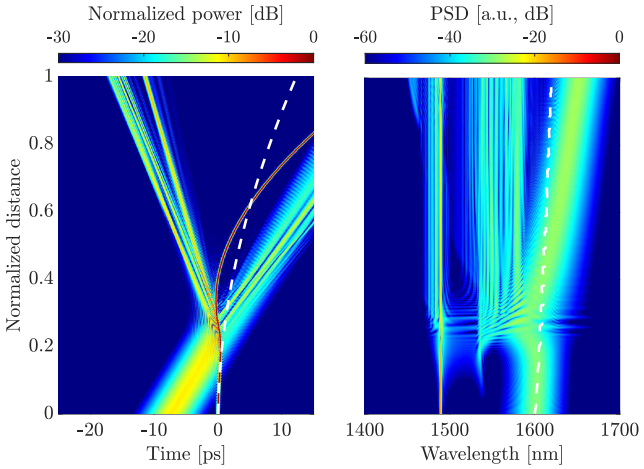

Fig. 3. Soliton and control pulse interaction in time (left) and frequency (right) domains, for $P_c = 20$ W, $\Delta T = -7.5$ ps, and ZNW = 1450 nm. The dashed white line shows the soliton evolution with no control pulse. Distance is normalized to the optical-fiber length and power is referred to the soliton's peak power P_0.

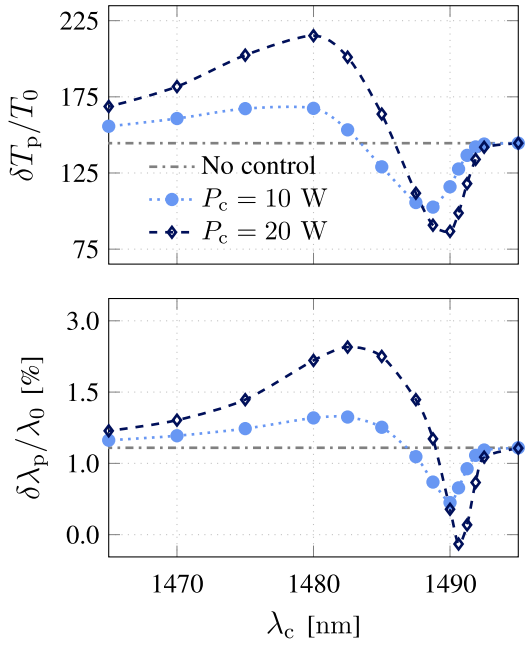

Fig. 4. Output time delay δT_p (top) and wavelength shift $\delta\lambda_p$ (bottom) of the soliton, normalized to the initial soliton width, T_0, and wavelength, λ_0 vs. control-pulse wavelength for $\Delta T = -20$ ps and ZNW = 1450 nm.

ZNW = 1450 nm (top) and ZNW = 1650 nm (bottom). Since there is no need for the control pulse to be a soliton, and by way of example, λ_c was chosen shorter than the ZDW. As it can be readily seen, the frequency shift changes monotonically with the control-pulse power P_c. Moreover, a much smaller shift is attained when ZNW = 1650 nm. Indeed, the ZNW acts as a barrier [33] and, thus, the control pulse exerts little effect on the soliton dynamics. In what follows we focus our attention on the case of ZNW = 1450 nm.

Pulse dynamics are portrayed in Fig. 3, which shows in the time (left) and in the frequency (right) domains the interaction for $P_c = 20$ W. For comparison, we show soliton dynamics with its corresponding time and frequency shifts caused by Raman without a control pulse, indicated with a dashed white line (cf. equation (5)). It can been seen that when a control pulse is launched, the soliton experiences an augmented redshift and delay. Moreover, the soliton does not undergo a fission upon collision. As it is explained in [16] using the space-time analogy, it is the control pulse which splits into a transmitted and a reflected beam. The reflected pulse wavelength lies in between that of the initial control pulse and the soliton, and its actual value depends on the initial control wavelength, λ_c, among other parameters.

To study the influence of control pulse parameters, we start by varying its wavelength, initially delayed a $\Delta T = -20$ ps with respect to the soliton. Results are shown in Fig. 4, both for the output soliton delay, δT_p (top), and wavelength shift, $\delta\lambda_p$ (bottom). We observe that both magnitudes increase with an increasing power of the control pulse. Furthermore, note that for a certain control pulse wavelength (e.g., $\lambda_c = 1491.25$ nm for $P_c = 20$ W), it is possible to restore the soliton wavelength back to its original value, therefore suppressing the effect of Raman.

It is interesting to compare RIFS suppression in the current scenario with that proposed by Arteaga-Sierra et al. [33] (see also [21]), where an intense pulse is launched at a wavelength shorter than the ZNW. As the pulse redshifts due to Raman, it 'hits the wall' of the zero-nonlinearity wavelength and no further frequency shifts are possible. However, the pulse is not restored to its original wavelength, as it does occur with the scheme proposed in this work. Furthermore, our approach is more flexible as it depends on adjusting some readily controllable parameters of a weak pulse, such as its power or delay.

Figure 5 shows the interaction for $\lambda_c = 1482.5$ nm (top) and 1491.25 nm (bottom), corresponding to the maximum positive and negative wavelength shifts, respectively, in both cases with $P_c = 20$ W (cf. Fig. 4). While in the former case the interaction of the control pulse with the soliton takes place midway down the fiber, in the latter it occurs close to the output end of the fiber, thus preventing any further Raman frequency shift.

Results shown in Fig. 5 can be explained as follows: The intense soliton acts as a temporal barrier for the control pulse and, in the case of a temporal reflection (strongly related to the control wavelength [16]), it is slightly blueshifted. Further, since control and soliton pulses are ~ 100 nm apart (close to the Raman peak gain in silica), there is an energy transfer from the control to the intense pulse mediated by Raman [2]. Given that the initial soliton wavelength lies close to the ZDW, it experiences a reduced second-order dispersion after being blueshifted. As explained in [34], the energy increase and reduction of dispersion need to be compensated by an increase in the peak power and a narrowing of the pulse in order to maintain the soliton condition (let us recall that the energy and width of a fundamental soliton are $E = \sqrt{P_0|\beta_2|/\gamma_0}$ and $T_0 = \sqrt{|\beta_2|/\gamma_0 P_0}$, respectively). This, in turn, leads to an enhanced Raman-induced redshift after the collision. Thus, by carefully selecting the control wavelength such that the interaction takes place close to the fiber input end, the soliton

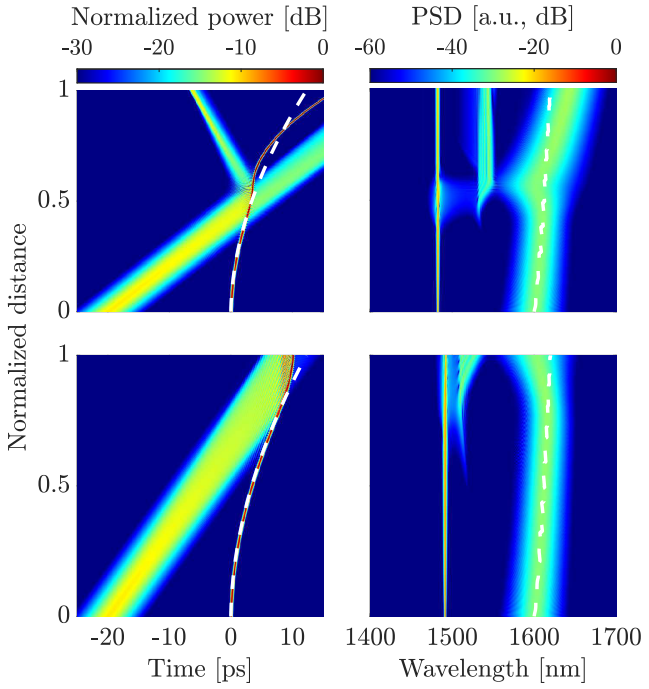

Fig. 5. Soliton and control pulse interaction in time (left) and frequency (right) domains, for $\lambda_c = 1482.5$ nm (top) and $\lambda_c = 1491.25$ nm (bottom), $P_c = 20$ W, $\Delta T = -20$ ps, and ZNW $= 1450$ nm. The dashed white line shows the soliton evolution with no control pulse. Distance is normalized to the optical-fiber length and power is referred to the soliton's peak power P_0.

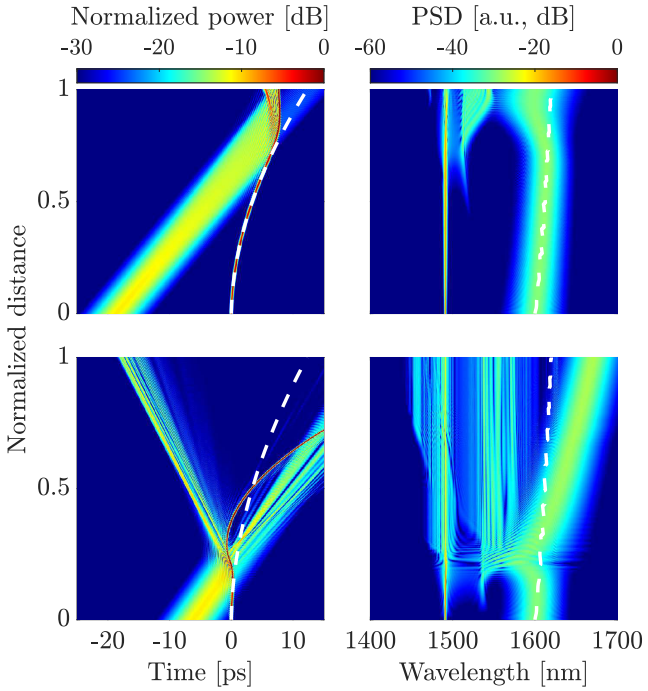

Fig. 6. Soliton and control pulse interaction in time (left) and frequency (right) domains, for $\Delta T = -18.75$ ps (top) and $\Delta T = -6.25$ ps (bottom), $P_c = 20$ W, $\lambda_c = 1491.25$ nm, and ZNW $= 1450$ nm. The dashed white line shows the soliton evolution with no control pulse. Distance is normalized to the optical-fiber length and power is referred to the soliton's peak power P_0.

will undergo an enhanced redshift for longer distances (cf. top of Fig. 5), whereas if the pulse collision occurs close to the fiber output end, the soliton will remain blueshifted (cf. bottom of Fig. 5). If the control wavelength is such that the control pulse is only slightly reflected, there is no observed blueshift and no enhanced redshift upon interaction. This limits the extent of the achievable frequency shift as only a range of control wavelengths yield the required reflection condition. All in all, the wavelength determines how much the control pulse is reflected and the Raman-mediated energy transfer to the soliton (and thus its blueshift), as well as where the interaction takes place along the fiber (and hence the extent of RIFS).

While the control-pulse wavelength bears influence in different concurring effects, changes to the initial delay between the control pulse and the soliton determine where along the fiber the interaction takes place, while maintaining the reflection condition required to attain significant changes of the soliton wavelength and delay. Figure 6 shows results for $\Delta T = -18.75$ ps (top) and -6.25 ps (bottom), $P_c = 20$ W, and $\lambda_c = 1491.25$ nm. As it can be observed, the soliton and the control pulse interact earlier for the shorter delay, leading to an enhanced redshift. Further, the soliton is blueshifted when the interaction occurs at the output end of the fiber, i.e., $\Delta T = -18.75$ ps. The effect of a varying initial delay on the wavelength shift and output delay of the soliton is shown in Fig. 7, where simulation parameters are those in Fig. 6, and $P_c = 10$ W and 20 W. Observe that the Raman shift can also be suppressed, this time by tuning the initial delay between the control pulse and the soliton.

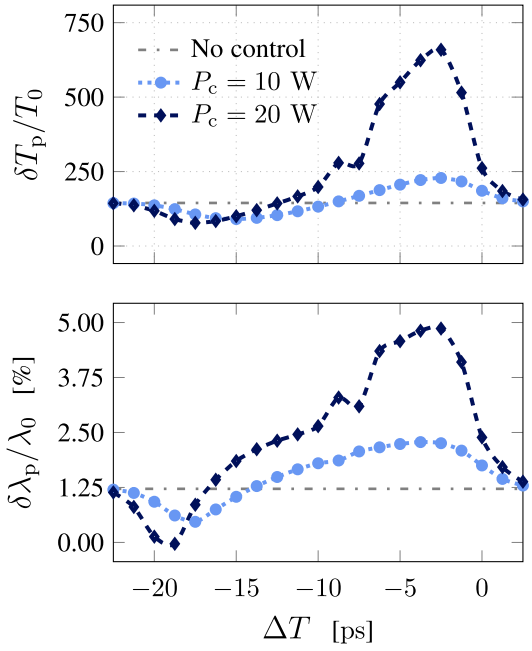

Fig. 7. Output time delay δT_p (top) and wavelength shift $\delta\lambda_p$ (bottom) of the soliton, normalized to the initial soliton width, T_0, and wavelength, λ_0 vs. control-pulse delay for $\lambda_c = 1491.25$ nm and ZNW $= 1450$ nm.

Results demonstrate that the central wavelength and the group delay of a soliton can be controlled in a precise manner by using a control pulse, and this feature can be applied in straightforward fashion to an all-optical switching scheme. For instance, using a bandpass filter or by properly selecting a time window, the soliton can be either transmitted

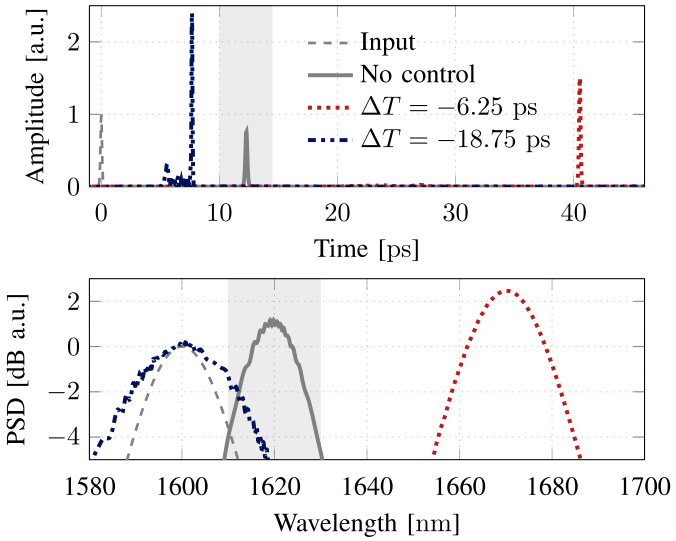

Fig. 8. Output in time (top) and frequency (bottom) domains, for $\Delta T = -6.25$ ps (dotted red) and $\Delta T = -18.75$ ps (dashed blue), $\lambda_c = 1491.25$ nm (bottom), $P_c = 20$ W, and ZNW = 1450 nm. The shaded-grey regions show the time window and a bandpass filter that enable all-optical switching schemes.

or blocked depending on the presence or absence of a carefully tuned control pulse. Figure 8 pictorially shows such a scheme for all-optical switching for two different initial delays, $\Delta T = -6.25$ ps and $\Delta T = -18.75$ ps. In the absence of a control pulse, the soliton lies within the transmission regions of the time and frequency filters (shown in shaded gray). When the control pulse is launched with $\Delta T = -18.75$ ps, while the RIFS suppression is clear, part of the soliton spectrum falls within the transmission region, which is not optimal condition for on-off switching. On the other hand, for the case with $\Delta T = -6.25$ ps, the enhanced redshift allows for a proper filtering of the output pulse, both in time and frequency.

IV. Conclusion

We studied the interaction between an intense soliton and a weak control pulse in media with a zero-nonlinearity wavelength (ZNW). By means of numerical simulations based on the photon-conserving NLSE, we showed that the soliton wavelength and delay can be modified by the proper choice of parameters of the control pulse, such as its power, wavelength, and initial delay. Further, the ZNW was shown to play a crucial role on the ensuing pulse dynamics. Most notably, we demonstrated that it is possible to completely suppress the soliton RIFS by allowing the pulse interaction to occur at the output end of the fiber. Conversely, if the pulse collision occurs early on along propagation the RIFS can be enhanced, enabled by the Raman-mediated energy transfer from the control pulse to the soliton. In all cases, observed phenomena were explained by relying on the temporal analogy of reflection and transmission. Finally, we proposed a straightforward all-optical switching scheme, based on time and frequency windows.

Acknowledgment

Alexis C. Sparapani gratefully acknowledges support from the Fulbright Commission and the Ministry of Education of Argentina for his stay at the University of Rochester where part of this work was carried out.

References

[1] G. P. Agrawal, *Fiber-Optic Communication Systems*. Hoboken, NJ, USA: Wiley, 2012.
[2] G. P. Agrawal, *Nonlinear Fiber Optics*, 6th ed., New York, NY, USA: Academic, 2019.
[3] S. Wabnitz and B. J. Eggleton, "All-optical signal processing," *Opt. Sci.*, vol. 194, no. 4, pp. 660–680, 2015.
[4] A. E. Willner, S. Khaleghi, M. R. Chitgarha, and O. F. Yilmaz, "All-optical signal processing," *J. Lightw. Technol.*, vol. 32, no. 4, pp. 660–680, Feb. 4, 2014.
[5] Y. Liu and H. W. M. Salemink, "Photonic crystal-based all-optical on-chip sensor," *Opt. Exp.*, vol. 20, no. 18, pp. 19912–19920, 2012.
[6] J. Belfi, G. Bevilacqua, V. Biancalana, Y. Dancheva, and L. Moi, "All optical sensor for automated magnetometry based on coherent population trapping," *J. Opt. Soc. Amer. B, Opt. Phys.*, vol. 24, no. 7, p. 1482, 2007.
[7] M. Fajkus, J. Nedoma, R. Martinek, V. Vasinek, H. Nazeran, and P. Siska, "A non-invasive multichannel hybrid fiber-optic sensor system for vital sign monitoring," *Sensors*, vol. 17, no. 1, p. 111, Jan. 2017.
[8] Z. Chai, X. Hu, F. Wang, X. Niu, J. Xie, and Q. Gong, "Ultrafast all-optical switching," *Adv. Opt. Mater.*, vol. 5, no. 7, 2017, Art. no. 1600665.
[9] V. R. Almeida et al., "All-optical switching on a silicon chip," *Opt. Lett.*, vol. 29, no. 24, p. 2867, 2004.
[10] K. Nozaki et al., "Sub-femtojoule all-optical switching using a photonic-crystal nanocavity," *Nature Photon.*, vol. 4, no. 7, pp. 477–483, Jul. 2010.
[11] Z. Deng, X. Fu, J. Liu, C. Zhao, and S. Wen, "Trapping and controlling the dispersive wave within a solitonic well," *Opt. Exp.*, vol. 24, no. 10, p. 10302, 2016.
[12] O. Melchert et al., "All-optical supercontinuum switching," *Commun. Phys.*, vol. 3, no. 1, pp. 1–8, Aug. 2020.
[13] W. Cai, Z. Yang, H. Wu, L. Wang, J. Zhang, and L. Zhang, "Effect of chirp on pulse reflection and refraction at a moving temporal boundary," *Opt. Exp.*, vol. 30, no. 19, p. 34875, 2022.
[14] A. Demircan, S. Amiranashvili, and G. Steinmeyer, "Controlling light by light with an optical event horizon," *Phys. Rev. Lett.*, vol. 106, no. 16, Apr. 2011, Art. no. 163901.
[15] J. Zhang, W. Donaldson, and G. P. Agrawal, "Impact of the boundary's sharpness on temporal reflection in dispersive media," *Opt. Lett.*, vol. 46, no. 16, pp. 4053–4056, 2021.
[16] B. W. Plansinis, W. R. Donaldson, and G. P. Agrawal, "What is the temporal analog of reflection and refraction of optical beams?" *Phys. Rev. Lett.*, vol. 115, no. 18, Oct. 2015, Art. no. 183901.
[17] B. W. Plansinis, W. R. Donaldson, and G. P. Agrawal, "Spectral splitting of optical pulses inside a dispersive medium at a temporal boundary," *IEEE J. Quantum Electron.*, vol. 52, no. 12, pp. 1–8, Dec. 2016.
[18] J. Zhang, W. R. Donaldson, and G. P. Agrawal, "Probing the decelerating trajectory of a Raman soliton using temporal reflection," *Opt. Exp.*, vol. 31, no. 17, p. 27621, 2023.
[19] A. Sparapani, G. Fernández, A. D. Sánchez, J. Bonetti, N. Linale, and D. F. Grosz, "All-optical pulse-train generation through the temporal analogue of a laser," *Opt. Fiber Technol.*, vol. 68, Jan. 2022, Art. no. 102785.
[20] S. Bose, A. Sahoo, R. Chattopadhyay, S. Roy, S. K. Bhadra, and G. P. Agrawal, "Implications of a zero-nonlinearity wavelength in photonic crystal fibers doped with silver nanoparticles," *Phys. Rev. A, Gen. Phys.*, vol. 94, no. 4, Oct. 2016, Art. no. 043835.
[21] F. R. Arteaga-Sierra, A. Antikainen, and G. P. Agrawal, "Soliton dynamics in photonic-crystal fibers with frequency-dependent Kerr nonlinearity," *Phys. Rev. A, Gen. Phys.*, vol. 98, no. 1, Jul. 2018, Art. no. 013830.
[22] S. Bose, R. Chattopadhyay, S. Roy, and S. K. Bhadra, "Study of nonlinear dynamics in silver-nanoparticle-doped photonic crystal fiber," *J. Opt. Soc. Amer. B, Opt. Phys.*, vol. 33, no. 6, p. 1014, 2016.
[23] S. Bose et al., "Role of frequency dependence of the nonlinearity on a soliton's evolution in photonic crystal fibers," *Opt. Lett.*, vol. 46, no. 16, pp. 3921–3924, 2021.
[24] S. M. Hernandez, A. Sparapani, N. Linale, J. Bonetti, D. F. Grosz, and P. I. Fierens, "Dispersive waves and radiation trapping in optical fibers with a zero-nonlinearity wavelength," *Waves Random Complex Media*, vol. 4, pp. 1–15, Jan. 2022.

[25] S. Zhao, R. Guo, and Y. Zeng, "Effects of frequency-dependent Kerr nonlinearity on higher-order soliton evolution in a photonic crystal fiber with one zero-dispersion wavelength," *Phys. Rev. A, Gen. Phys.*, vol. 106, no. 3, Sep. 2022, Art. no. 033516.

[26] A. C. Sparapani, J. Bonetti, N. Linale, S. M. Hernandez, P. I. Fierens, and D. F. Grosz, "Temporal reflection and refraction in the presence of a zero-nonlinearity wavelength," *Opt. Lett.*, vol. 48, no. 2, p. 339, 2023.

[27] G. P. Agrawal, *Nonlinear Fiber Optics*. Amsterdam, The Netherlands: Elsevier, 2019.

[28] K. J. Blow and D. Wood, "Theoretical description of transient stimulated Raman scattering in optical fibers," *IEEE J. Quantum Electron.*, vol. 25, no. 12, pp. 2665–2673, Dec. 1989.

[29] J. Bonetti, N. Linale, A. D. Sánchez, S. M. Hernández, P. I. Fierens, and D. F. Grosz, "Photon-conserving generalized nonlinear Schrodinger equation," *J. Opt. Soc. Amer. B, Opt. Phys.*, vol. 37, no. 2, pp. 445–450, 2020.

[30] S. M. Hernández, J. Bonetti, N. Linale, D. F. Grosz, and P. I. Fierens, "Soliton solutions and self-steepening in the photon-conserving nonlinear Schrodinger equation," *Waves Random Complex Media*, vol. 32, no. 5, pp. 1–17, 2020.

[31] N. Linale, P. I. Fierens, and D. F. Grosz, "Revisiting soliton dynamics in fiber optics under strict photon-number conservation," *IEEE J. Quantum Electron.*, vol. 57, no. 2, pp. 1–8, Apr. 2021.

[32] N. Linale, P. I. Fierens, J. Bonetti, A. D. Sánchez, S. M. Hernandez, and D. F. Grosz, "Measuring self-steepening with the photon-conserving nonlinear Schrodinger equation," *Opt. Lett.*, vol. 45, no. 16, pp. 4535–4538, 2020.

[33] F. R. Arteaga-Sierra, A. Antikainen, and G. P. Agrawal, "Raman-shift suppression and soliton splitting in photonic crystal fibers with nonlinear dispersion," in *CLEO: QELS_Fundamental Science*. Washington, DC, USA: Optica Publishing Gro, 2017.

[34] A. Demircan, S. Amiranashvili, C. Brée, U. Morgner, and G. Steinmeyer, "Supercontinuum generation by multiple scatterings at a group velocity horizon," *Opt. Exp.*, vol. 22, no. 4, p. 3866, 2014.

Alexis C. Sparapani (Member, IEEE) received the Electronic Engineering degree from Universidad Tecnológica Nacional (UTN), Argentina, in 2019, and the Ph.D. degree from Instituto Balseiro, UNCuyo, Argentina, in 2024. His research interests include nonlinear optics and communications. He was a recipient of the Fulbright Scholarship.

Lucas N. Gutierrez received the Licenciado degree in physics from Universidad de Buenos Aires (UBA), Argentina, in 2023. He is currently pursuing the Ph.D. degree with Instituto Balseiro, UNCuyo, Argentina. His research interests include nonlinear optics and communications.

Santiago M. Hernandez received the Electronic Engineering and Ph.D. degrees from Instituto Tecnológico de Buenos Aires (ITBA), Argentina, in 2001 and 2012, respectively. He is currently with the Optical Communications Group, Departamento de Ingeniería en Telecomunicaciones, Comisión Nacional de Energía Atómica (CNEA), Argentina, and a Researcher with Consejo Nacional de Investigaciones Científicas y Técnicas (CONICET), Argentina. His research interests include control theory and modeling of nonlinear optical propagation.

Pablo I. Fierens (Senior Member, IEEE) received the Electronic Engineering degree from Instituto Tecnológico de Buenos Aires (ITBA), Argentina, in 1997, and the M.Sc. and Ph.D. degrees from Cornell University, USA, in 2000 and 2003, respectively. He is currently with the Optoelectronics Center, ITBA, and a Researcher with Consejo Nacional de Investigaciones Científicas y Técnicas (CONICET), Argentina. He is interested in communications, nonlinear optics, complex networks, and noise in nonlinear systems.

Diego F. Grosz received the Licenciado degree in physics from Universidad de Buenos Aires (UBA), Argentina, in 1993, and the Ph.D. degree from Universidade Estadual de Campinas (Unicamp), Brazil, in 1998. He is currently with the Optical Communications Group, Departamento de Ingeniería en Telecomunicaciones, Comision Nacional de Energía Atomica (CNEA), Argentina, and a Researcher with Consejo Nacional de Investigaciones Científicas y Técnicas (CONICET), Argentina. His research interests include nonlinear and quantum optics and fiber-optic communication systems.

Govind P. Agrawal (Life Fellow, IEEE) received the M.S. and Ph.D. degrees from Indian Institute of Technology, New Delhi, in 1971 and 1975, respectively.

After holding positions with the école Polytechnique, France, the City University of New York, and Bell Laboratories, Murray Hill, NJ, USA. In 1989, he joined the Faculty of the Institute of Optics, University of Rochester, where he is currently a James C. Wyant Professor of optics. He is the author or co-author of ten books and more than 500 research publications. His books on *Nonlinear Fiber Optics* (Academic Press, 6th Edition, 2019) and *Fiber-Optic Communication Systems* (Wiley, 5th Edition, 2021) are used worldwide for research and teaching. His research interests include optical communications, nonlinear optics, and silicon photonics. He is a fellow of *Optica* (formerly OSA). He was a recipient of the IEEE Journal of Quantum Electronics Award in 2012, the Esther Hoffman Beller Medal in 2015, the OSA Max Born Award in 2019, and the Eps Quantum Electronics and Optics Medal in 2019. He was given the Lifetime Achievement Award of the University of Rochester in 2020. He was the Editor-in-Chief of *Advances in Optics and Photonics* from 2014 to 2019. He is also a Distinguished Fellow of the Optical Society of India.